Inhibitory Effect of Commercial Inhibitor VCI 379/611 on the Corrosion Behaviour of HTCS-130 Tool Steel for Hot Work

Brajčinović, Sandra; Begić Hadžipašić, Anita; Medved, Jožef

Download date / Datum preuzimanja: **2024-07-23**

MDPI

Article

Inhibitory Effect of Commercial Inhibitor VCI 379/611 on the Corrosion Behaviour of HTCS-130 Tool Steel for Hot Work

Sandra Brajčinović [1], Anita Begić Hadžipašić [1,*] and Jožef Medved [2]

[1] Faculty of Metallurgy, University of Zagreb, Aleja Narodnih Heroja 3, 44000 Sisak, Croatia; smitic@simet.unizg.hr
[2] Faculty of Natural Sciences and Engineering, University of Ljubljana, Aškerčeva Cesta 12, 1000 Ljubljana, Slovenia; jozef.medved@ntf.uni-lj.si
* Correspondence: begic@simet.unizg.hr

Abstract: This paper presents the results of a study of the influence of water and the commercial inhibitor VCI 379/611 on the corrosion behaviour of HTCS-130 hot work tool steel. Using the thermodynamic program Thermo-Calc, phase equilibria were determined according to the choice of calculation conditions and the known chemical composition of tool steels. From the obtained projections, it is possible to observe the secretion of individual phases at certain temperatures. To obtain insight into the corrosion resistance of steel, the following electrochemical methods were used: open circuit potential measurement; electrochemical impedance spectroscopy; and Tafel extrapolation. Metallographic tests were performed on a sample previously etched in nital to identify the microstructure of the steel. Using an optical microscope, the sample surface was analysed after each measurement. Images of the sample surface subjected to water without inhibitors indicate the occurrence of pitting corrosion. The presence of tungsten and molybdenum carbides was identified by scanning electron microscopy and energy dispersion spectroscopy. It was found that the corrosion process is more pronounced in the area of the metal base while in the areas of excreted carbides, weaker corrosion activity was observed.

Keywords: hot work tool steel; electrochemical techniques; corrosion parameters; microstructure; phase equilibria

1. Introduction

Today, steel is the most important structural material in almost all fields of technology. Its wide application is based on its outstanding properties such as high strength, hardness, ductility, thermal conductivity, elasticity, and corrosion resistance [1–4]. Its properties can be changed by alloying, heat and surface treatment, and cold forming [1–5]. It can be formed in hot or cold conditions, by rolling, forging, pressing, etc. Due to all the above, steel can be adapted to different purposes, which is why it is considered affordable and relatively cheap when compared to other materials. Steel can be divided according to several bases and the most common division is according to the composition of carbon and alloy steel. It can also be divided according to the microstructure, properties, production method, and purpose [1–4]. According to the purpose, steels are divided into structural, tool, and special purpose steels.

In industrial plants, the use of tools is becoming ever more present. Modern industrial development strives towards mass production, with enhanced reliability of machines and tools used to be expected. Tool steels are divided into carbon tool steels, cold work tool steels, hot work tool steels, and high-speed steels [1–5].

Structural alloys with improved properties include tool steels for hot work that are most often exposed to high or elevated temperatures, and subjected to various loading and wear processes, and they require maximum durability with minimal maintenance [6,7]. Due to their exceptional strength, tool steels are well adapted for the production of high-pressure

die-casting moulds, various impact tools, and turning blades and cutting tools, such as drills, blades, and saw blades [8]. Therefore, it is very important to achieve structural stability and good mechanical and corrosion properties.

Various forms of corrosive damage and the formation of cracks, which lead to material breakage, are constantly present in many materials, especially metals, and thus in tool steels [9–13]. Due to corrosion, a large part of the metallic material deteriorates irreversibly, which is why recent scientific research has focused on designing innovative metallic materials with an optimal chemical composition and microstructure, which show a better corrosion resistance under application conditions. Many authors have studied the corrosion behaviour of steels in different media and application conditions and the possibilities of their anti-corrosion protection (cathodic protection, protective coatings, inhibitors, etc.) [14–19]. May [14] studied the influence of different immersion times and different concentrations of NaCl solution on the corrosion behaviour of mild steel. The kinetics of corrosion behaviour was investigated using the weight loss method. He came to the conclusion that the corrosion behaviour of mild steel is influenced by dissolved oxygen and chloride ions, which are very aggressive, which accelerates the anodic reaction and contributes to faster dissolution of the metal. Fekry and Ameer [15] investigated the rate of development of mild steel hydrogen in sulphuric acid solution. Using electrochemical techniques (EIS, polarisation curves), they concluded that the corrosion rate of mild steel decreases with an increasing concentration of the inhibitor in sulphuric acid solution. In recent times, increasingly more attempts have been made to replace harmful inhibitors with those that are environmentally friendly to protect ecosystems and human health. Thus, Abdel-Gaber et al. [18] studied the inhibitory effect of some plant extracts on the corrosion behaviour of steels in acidic media. They found that the tested plant extracts acted as mixed inhibitors and showed a very high efficiency in reducing the corrosion rate. The inhibitory effect is explained by the theory of the adsorption of stable complexes on the surface of the tested steel. Franceschi et al. [20] studied the impact of different austempering heat treatments on the corrosion behaviour of high-silicon steel and found that the corrosion resistance of the tested samples of high-silicon steel increased with the increasing volume fraction of residual austenite due to the reduced amount of residual stress. Namely, silicon slowed down the precipitation of carbides into cementite, which then increased the stability of austenite and its retention at room temperature. To obtain an optimal microstructure, such steels need to be subjected to a specific heat treatment consisting of several steps. The main purpose of such heat treatment is to obtain a microstructure consisting of residual austenite and free carbide bainite, which contributes to the high strength of the material and higher hardness than martensite.

HTCS-130 hot work tool steels belong to the group of tool steels intended for operation at temperatures higher than 200 °C. This group of steels, in cast or heat-treated conditions, requires high hardness and wear resistance, temperature stability, and strength resistance at elevated temperatures [21,22]. During application, tool steels are exposed to contact stress, bending stress, twisting stress, impact loading, and thermal fatigue. The operating temperatures of tool steels increase to 600 °C and may cause material structural changes, affecting the strength and thermal stability at elevated temperatures [23,24]. The alloying elements are used to improve the corrosion resistance, particularly at high temperatures. The main alloying elements that are part of this steel group are: chromium; molybdenum; and vanadium; and often tungsten is added as well. The main reason the alloying elements are added is the formation of the carbides, providing a greater wear resistance and resistance to tempering [25,26]. The problems in the use of tool steel for hot work production are related to the temperature increase, which can lead to a reduction in the hardness, microstructural changes, and thermal fatigue [27,28]. The amount of carbide is determined by the content of carbon and alloying elements. Carbide phases are usually oval, although angular carbides may appear within the structure, negatively affecting the tool steel properties [29]. Large carbide phase clusters along the grain boundaries negatively affect the tool properties.

Therefore, we aimed to achieve a fine-grained carbide cell structure at the grain boundaries to achieve greater resistance to breaking and the formation of cracks [30,31].

In this paper, research was conducted on a group of tool steels (designation HTCS-130) intended for hot work. The purpose of this paper was to study the corrosion behaviour of HTCS-130 hot work tool steel and to evaluate whether the VCI 379/611 inhibitor was effective at slowing down the corrosion of investigated steel. Moreover, the aim of this research was to connect the results of the corrosion research with the chemical composition and microstructure of HTCS-130 tool steel for hot work. Therefore, the Thermo-Calc thermodynamic calculation program was used, utilising the CALPHAD principle, with the phase equilibria established according to the selection of the budget and the known tool steel chemical composition. By applying electrochemical tests in water and with different additions of inhibitor, the corrosion parameters of the tested steel were obtained and compared. Metallographic tests confirmed the types of carbides and their influence on the corrosion behaviour of the tested tool steel, and the influence of the chemical composition on the corrosion behaviour of the tested tool steel.

2. Experimental Part

2.1. Materials

Table 1 shows the chemical composition of HTCS-130 hot work tool steel.

Table 1. Chemical composition of the tested HTCS-130 hot work tool steel (mas. %).

C	S	Si	Cr	Ni	V	W	Co	Al	Fe
0.31	0.001	0.07	0.1	0.04	0.01	1.9	0.01	0.012	
Cu	**Mn**	**Mo**	**P**	**Sn**	**Ti**	**Nb**	**B**	**N**	balance
0.04	0.08	3.2	0.007	0.005	0.01	0.01	0.001	0.001	

This tool steel contains a higher percentage of alloying elements such as tungsten and molybdenum. Molybdenum and tungsten have a high affinity for carbon and form stable carbides. Tungsten and molybdenum carbides increase steel's wear resistance. They also contribute to increased strength at elevated temperatures, harden ferrite, and increase hardenability [25]. The amount of undesirable impurities in the tested steel (silicon, nitrogen, phosphorus, sulphur) was within a permissible range.

2.2. Sample Preparation

Tool steel samples were cut and prepared pressed into a conductive mass using a hot pressing device (SimpliMet® 1000, manufacturer: Büehler, Lake Bluff, IL, USA) and then machine-ground on an automatic device PhenixBeta Grinding/Polisher with Vector LC Power Head (manufacturer: Büehler, Lake Bluff, IL, USA). Grinding was carried out using sandpaper with gradation Nos. 240, 400, 600, and 800. A suspension of Al_2O_3 in water was used for polishing. The prepared samples were washed in distilled water and degreased in ethanol. One prepared sample was set aside for etching in nital for the purpose of recording the microstructure, and the other was intended for electrochemical measurements.

2.3. Thermodynamic Calculations

Using the program Thermo-Calc and database TCFE 10, which works on the principle of the CALPHAD method, the phase equilibria were determined according to the choice of calculation conditions and the known chemical composition of tool steels [32,33]. According to a certain area, the temperatures and phases segregated at these temperatures were recorded from the phase diagram.

2.4. Electrochemical Tests (E_{corr}, EIS, Tafel)

The E_{corr} corrosion potential method, electrochemical impedance spectroscopy (EIS), and Tafel extrapolation method were used to obtain data on the corrosion behaviour of the samples. Electrochemical measurements were performed at room temperature (19 ± 2) °C using a potentiostat/galvanostat (Parstat 2273, manufacturer: Ametek, Leicester, UK) and a computer, which recorded the data during the measurement. The measuring apparatus consisted of a three-electrode glass cell (Figure 1).
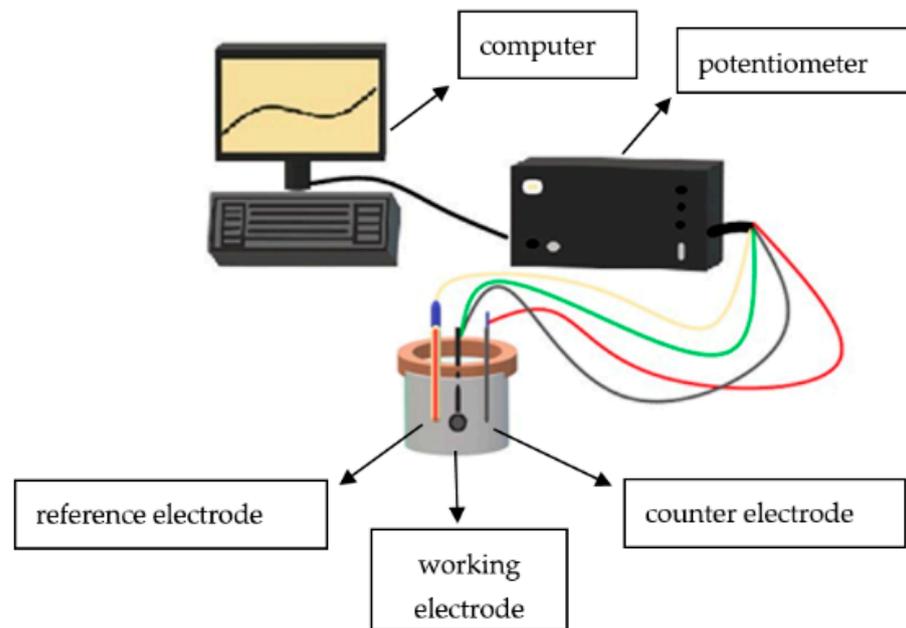

Figure 1. Apparatus for electrochemical measurements.

The working electrode was a test sample of steel that was immersed in the working medium (volume 200 mL). A saturated calomel electrode was used as a reference electrode, and a platinum electrode was used as a counter electrode [34]. So, the potential values are presented relative to the saturated calomel electrode. During the measurement, the sample was exposed to ordinary water and to a prepared solution of distilled water with the addition of a commercial inhibitor in different percentages.

Using the method of determining the corrosion potential of E_{corr}, data on the corrosion behaviour of the sample during exposure in different media was obtained. The measurements were performed by keeping the circuit between the working electrode and the counter electrode open for the purpose of measuring the potential difference between the working electrode and the counter electrode. The measurement was performed in a time period of 1800 s.

The electrochemical impedance spectroscopy measurements were performed in the frequency range from 100 kHz to 10 mHz, and the amplitude of the sinusoidal voltage was 5 mV. The impedance parameters were analysed using ZSimpWin 3.60 software (EChem Sotfware, creator: Bruno Yeum, Ph.D., Ann Arbor, MI, USA) with the selection of the appropriate model of the electrical circuit *R(Q(R(QR)))*.

Potentiodynamic polarisation tests were performed in the potential range from −250 to +250 mV vs. E_{corr}. The rate of potential change was 1 mV/s. Using the PowerCorrTM software and PowerSuite software 2.58 (creator: Ametek, Leicester, UK), the corrosion parameters (corrosion potential E_{corr}, corrosion rate v_{corr}, anodic slope b_a, and cathode slope b_c) were obtained.

The efficiency coefficient Z [9,18] was calculated from the data on the corrosion current density in the solution without inhibitor and with inhibitor using Equation (1):

$$Z = \frac{I_{corr} - I_{corr}^{inh}}{I_{corr}} \cdot 100 \tag{1}$$

where I_{corr} is the corrosion current density without an inhibitor, and I_{corr}^{inh} is the corrosion current density with an inhibitor.

Each of the above-described electrochemical measurements were repeated three times to assure statistical reproducibility.

2.5. Preparation of Solutions

Commercial inhibitor concentrate VCI 379/611 was used for testing. When mixed with water, the VCI 379/611 inhibitor is intended as an additive for the preservation of metal elements in covered warehouses. Its chemical composition is based on sulfonates and additives of volatile corrosion inhibitors. It is soluble in water and forms a transparent layer with water. It is applied on metal surfaces via spraying or immersion. For the purpose of the examination, the inhibitor was mixed with distilled water at a ratio of 1%, and then, in the second measurement, the addition of the inhibitor was diluted. This was carried out by making a 50:50 solution of distilled water and inhibitor. A 1% sample was then taken from the prepared ratio and mixed with distilled water. In the following, for ease of interpretation, the solution with the addition of 1% inhibitor is designated as solution 1 while the solution with the addition of the diluted inhibitor is designated as solution 2.

2.6. Metallographic Examinations

Metallographic tests were performed on a light microscope with a digital camera (Olympus GX 51, manufacturer: Olympus, Tokyo, Japan) and an automatic image processing system (AnalySIS® Materials Research Lab, manufacturer: Olympus, Tokyo, Japan). The scanning electron microscope (Tescan Vega LSH (TS 5130 LS), manufacturer: Tescan Vega, Brno, Czech Republic) recorded the condition of the sample surface after etching in nital using a secondary electron detector at an accelerating voltage of 20 kV and spectral acquisition time of 45 s. The analysis was performed using an energy dispersion spectrometer to determine the elemental composition of the observed sample [35].

3. Results and Discussion

3.1. The Results of Thermodynamic Calculation

Using the Thermo-Calc program, a thermodynamic equilibria isopleth phase diagram was calculated according to the chemical composition (Figure 2).

Table 2. List of the stable phases from the calculation of the phase diagram using the Thermo-Calc method.

List of Phases Using Thermo—Calc Method	Standard Phases
LIQUID + BCC_A2	L + δ
LIQUID + BCC_A2 + FCC_A1	L + δ + γ
LIQUID + FCC_A1	L + γ
FCC_A1	γ
FCC_A1 + M6C	γ + (Mo, Fe, W)$_6$C
BCC_A2 + FCC_A1 + M6C	α + γ + (Mo, Fe, W)$_6$C
BCC_A2 + FCC_A1 + M6C + MC_SHP	α + γ + (Mo, Fe, W)$_6$C + (W, Mo)C
BCC_A2 + HCP_A3#2 + M6C + MC_SHP	α + (Mo, W, V)$_2$C + (Mo, Fe, W)$_6$C + (W, Mo)C
BCC_A2 + HCP_A3#2 + M6C + MC_ETA + MC_SHP	α + (Mo, V, W)$_2$C + (Mo, Fe, W)$_6$C + (Mo, V)C + (W, Mo)C

Figure 2. Isopleth phase diagram of HTCS-130 hot work tool steel.

According to the above projections, phase diagrams were constructed showing the segregation of individual phases at certain temperatures. Table 2 lists the individual phases in a particular area from the obtained phase diagram. The standard names of individual phases are given.

According to the obtained results, the equilibrium liquidus temperature of the tool steel HTCS-130 was 1503 °C, and solidus was 1421 °C. At a temperature of 1094 °C, the segregation of M_6C carbide occurred, with MC carbide segregating at 809 °C and M_2C carbide at 391 °C. $M_{23}C_6$ carbide segregation was recorded at 367 °C.

3.2. Electrochemical Investigations

Figure 3 shows that in the sample that was exposed to water, the open circuit potential tended towards negative values ($E = -406$ mV).

Figure 3. Time dependence of the open circuit potential of HTCS-130 tool steel in water, solution 1, and solution 2.

Thus, the extremely negative potential values indicate the instability of the sample in water. In solution 1, the stability of the sample was the same throughout the whole measurement, and the open circuit potential moved towards more positive values ($E = -29.1$ mV). In solution 2, the results were slightly worse compared to the measurement in solution 1 ($E = -38.5$ mV).

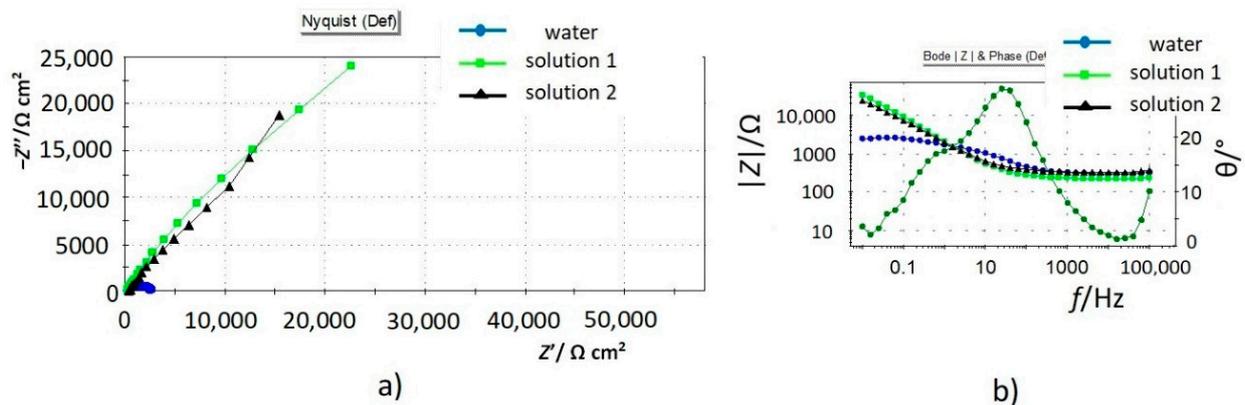The results of the electrochemical impedance spectroscopy are shown by the Nyquist and Bode diagram (Figure 4).

Figure 4. The comparative view of: (**a**) Nyquist's EIS diagrams and (**b**) Bode plots obtained for HTCS-130 tool steel in water, solution 1, and solution 2.

An example of the modelling of the electrical circuit is shown in Figure 5 for solution 1. According to the same principle of processing the results, modelling was performed for solution 2 and water.
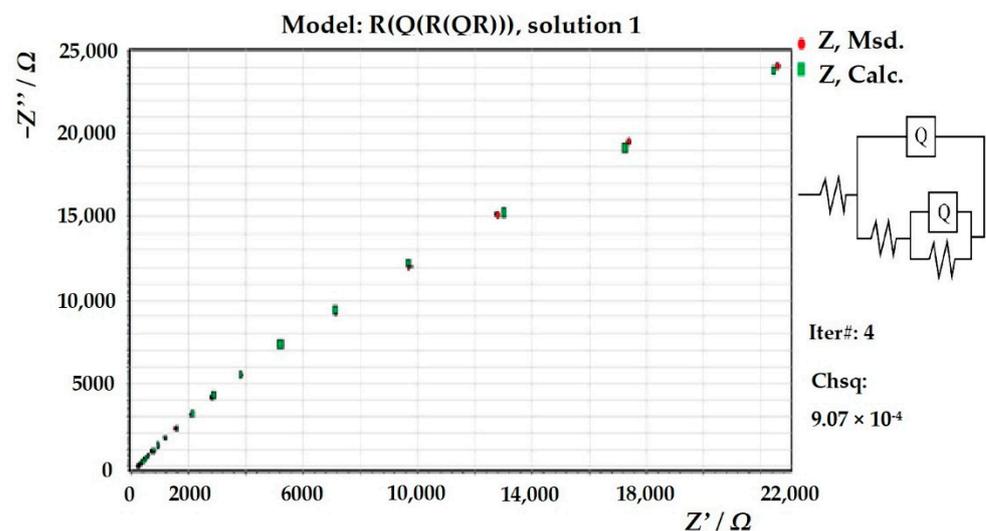
Figure 5. Modelling of Nyquist's EIS diagrams obtained for HTCS-130 tool steel in solution 1.

Table 3 lists the obtained impedance parameters.

The obtained Nyquist EIS spectra represent the dependence of the imaginary impedance on the real impedance for each measured frequency. From the modelled EIS spectra, it can be seen that the simulated curves match with the experimental ones well because a deviation of the order of 10^{-4} was registered, and the measurement error was less than 5%, which is an acceptable value. This shows that the R(Q(R(QR))) model was selected as the best fitting model of the electrical equivalent circuit. The choice of the equivalent circuit is in accordance with the shape of the Bode plot and with the data from the literature regarding the occurrence of oxide layers on the steel surface [34–37].

Table 3. Impedance parameters of the tested HTCS-130 tool steel.

Medium	E_{corr} vs. SCE	R_{el}	$Q_{dl} \times 10^6$	n	R_{ox}	$Q_{dl} \times 10^6$	n	R_{ct}
	mV	$\Omega\,cm^2$	$\Omega^1 s^n cm^{-2}$		$\Omega\,cm^2$	$\Omega^1 s^n cm^{-2}$		$\Omega\,cm^2$
water	−406	304.6	42.09	0.71	1339	458.7	0.78	1106
solution 1	−29.1	231.0	142.1	0.69	53,000	96.82	0.50	125,800
solution 2	−38.5	333.3	163.3	0.65	40,560	250.9	0.86	84,520

The Nyquist impedance representation of the sample in water is in the form of a depressed semicircle centred above the real axis. However, the tested sample in the water medium with the addition of inhibitor showed a tendency to form a straight line. The increase in the area on the Nyquist display indicates the higher inhibitor efficacy. This is confirmed by the data in Table 3.

A higher oxide resistance R_{ox} and charge transfer resistance R_{ct} were observed in the tool steel sample exposed to solution 1. The obtained results indicate that a thicker protective layer on the sample surface most likely formed during the test in solution 1. The lowest amounts of R_{ox} and R_{ct} were recorded for the sample during exposure to water, which means that an insufficient amount of film formed on the sample to act as a barrier and protect the steel from the action of aggressive ions in the solution [38].

The obtained results on the corrosion behaviour of HTCS-130 tool steel in water, solution 1, and solution 2 were also confirmed using the Tafel extrapolation method. The corrosion parameters of the tested HTCS-130 tool steel are shown in Table 4.

Table 4. Corrosion parameters of the tested HTCS-130 tool steel.

Medium	E_{corr} vs. SCE	b_a	b_c	I_{corr}	v_{corr}	Z
	mV	mV dec^{-1}	mV dec^{-1}	Acm^{-2}	mm yr^{-1}	%
water	−405.60	498.23	483.08	12.59×10^{-6}	0.804	0
solution 1	−129.26	1899.0	180.61	1.00×10^{-6}	0.080	90.04
solution 2	−151.56	699.1	180.38	1.26×10^{-6}	0.138	82.74

Figure 6 shows the polarisation curves of the tested HTCS-130 tool steel sample in water, solution 1, and solution. 2.

The graph has a semi-logarithmic form (E—log$I$), in which the logarithm of the current density is on the *x*-axis and the potential is on the *y*-axis.

From the obtained results, it was observed that for the sample tested in water, a higher corrosion rate was recorded compared to solution 1 and solution 2. By adding a different amount of inhibitor, the goal was to achieve a lower corrosion rate for HTCS-130 steel. The results obtained from the test in water with the addition of dilute inhibitor were very good. However, optimal results were recorded only from the test in distilled water with the addition of 1% commercial inhibitor.

From the obtained results, it can be concluded that in this case, the VCI 379/611 inhibitor is an anodic inhibitor. Namely, in solutions 1 and 2, the anodic polarisation is more pronounced, and the corrosion potential is shifted towards more positive values [9,14,36]. The addition of inhibitors reduced the corrosion current density. It is important to note that both the potentiodynamic polarisation tests and the EIS tests were performed after 30 min of open circuit stabilisation.
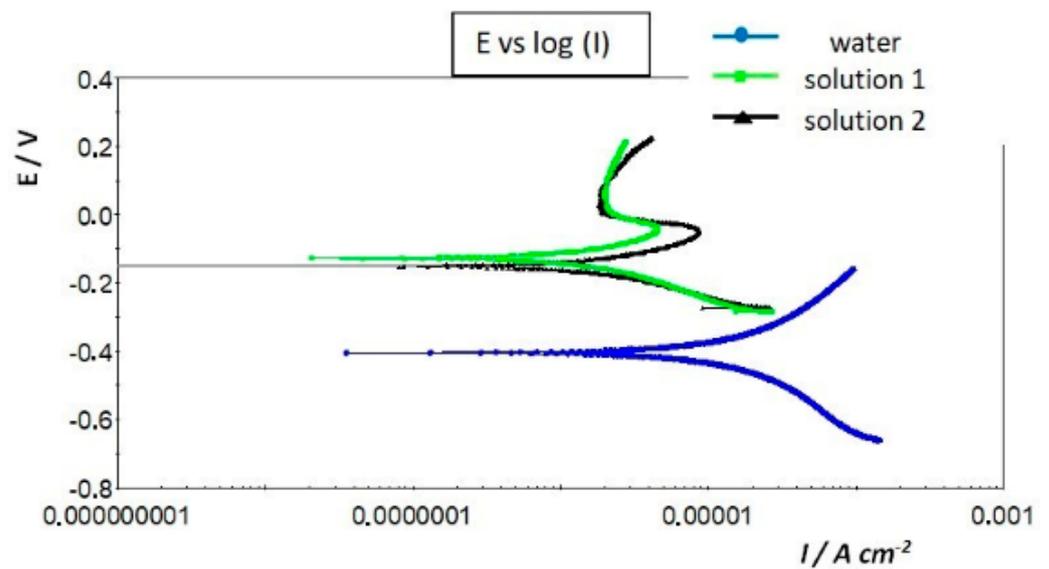
Figure 6. Polarisation curves of the tested HTCS-130 tool steel in water, solution 1, and solution 2.

3.3. Results of Metallographic Investigations

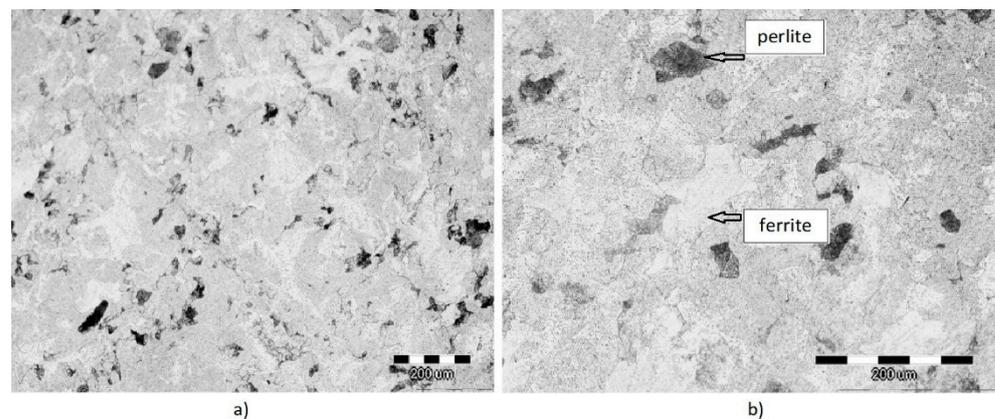Figure 7 shows metallographic images of the heat-treated HTCS-130 tool steel after etching in nital.

Figure 7. Microstructure of HTCS-130 hot work tool steel after etching in nital: (**a**) magnification 100× and (**b**) magnification 200×.

Metallographic analysis identified the ferrite-perlite structure. The structure of ferrite is highlighted in white and perlite in a darker colour [26,27,39]. The tested steel is characterised by high purity and a fine homogeneous structure. Moreover, the samples were recorded using scanning electron microscopy and analysis was performed using an energy dispersion spectrometer (Figure 8).

After SEM analysis, the presence of a ferrite-perlite phase in the steel was confirmed. Perlite is in the form of lamellar tiles. EDS analysis revealed the presence of tungsten and molybdenum (Table 5). These alloying elements are strong carbide-forming elements and form carbides of the Mo_6C and W_6C type, which are excreted as fine-grained carbides at the grain boundaries and slow down the corrosion process [6,26,40]. Balasko et al. [40] studied the high-temperature oxidation of four different types of tool steels for hot work, including HTCS-130 tool steel. HTCS-130 was shown to be the most resistant at 700 °C due to the good combination of alloying elements and a high molybdenum content, which improves the high-oxidation corrosion resistance.
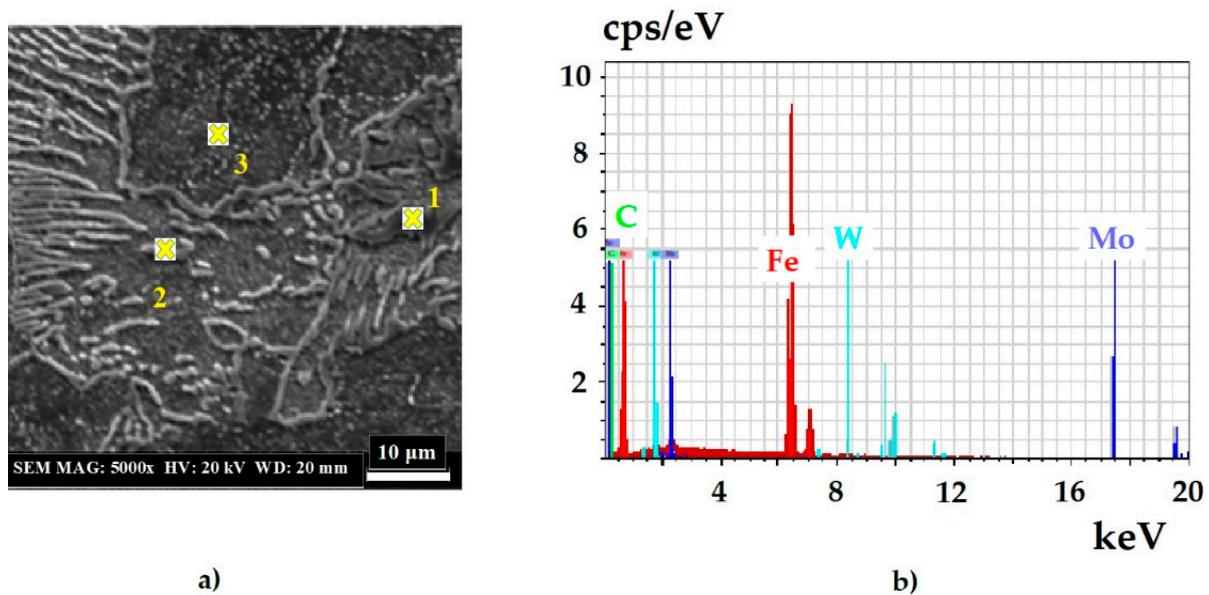
Figure 8. (**a**) SEM micrograph of the HTCS-130 hot work tool steel surface after etching in nital (magnification 5000×), (**b**) example of EDS analysis of position number 2.

Table 5. EDS analysis of the positions marked as 1, 2, and 3 in Figure 8a.

Position	Chemical Element, Mass. %			
	Fe	C	Mo	W
1	91.45	1.82	3.28	3.44
2	91.09	1.12	3.40	4.40
3	90.89	1.10	3.56	4.45

Figure 9 shows metallographic images of the sample after the electrochemical tests.

An accumulation of corrosion products was observed on the sample only exposed in water. According to the appearance of corrosion damage, the assumption is that it is pitting corrosion caused by the decomposition of a passive corrosion film that is not compact enough to be rebuilt [9,14,34,35]. Small anode sites corrode rapidly due to a lack of oxygen to protect the entire surface. As a result, potential differences are created between the metal surface and within the pits. The accumulation of aggressive ions from the solution is a problem, as greater destruction of the material can occur. The surface of the sample after the electrochemical tests in water with the addition of inhibitors remained unchanged. The inhibitor agent left a very thin transparent, dry film on the metal surface. The inhibitor concentrate used was formulated on the basis of thixotropic calcium sulfonate inhibitors. Calcium sulfonate is used as a thickener in the food and packaging industry. It is used as a protective layer against the formation of corrosion products.

Based on all of the above, it is concluded that the 1%VCI 379/611 inhibitor can be used to protect HTCS-130 tool steel for hot work from corrosion because it showed excellent efficiency (>90%) in reducing the corrosion rate of tested steel. Further dilution of the inhibitor did not show the same or greater efficacy. Therefore, 1% is the optimal amount of VCI 379/611 inhibitor to be added. The excellent efficiency was confirmed by metallographic tests of the sample surface after the corrosion tests, which found that testing in water without the addition of inhibitors led to pitting corrosion on the sample of HTCS-130 tool steel for hot work while surface tests after the corrosion tests in solution with the addition of 1% of inhibitors did not show changes in the appearance of the sample surface. This means that the 1% inhibitor used protected the sample surface from aggressive

ions, because it adsorbed on the sample surface and formed a protective film [18,34,35]. Corrosion attacks on the sample tested in water were more pronounced on a metal basis while in the areas of excreted carbides, weaker corrosion activity was observed. This means that the proven presence of tungsten and molybdenum carbides slows down the corrosion process [29,35,40].
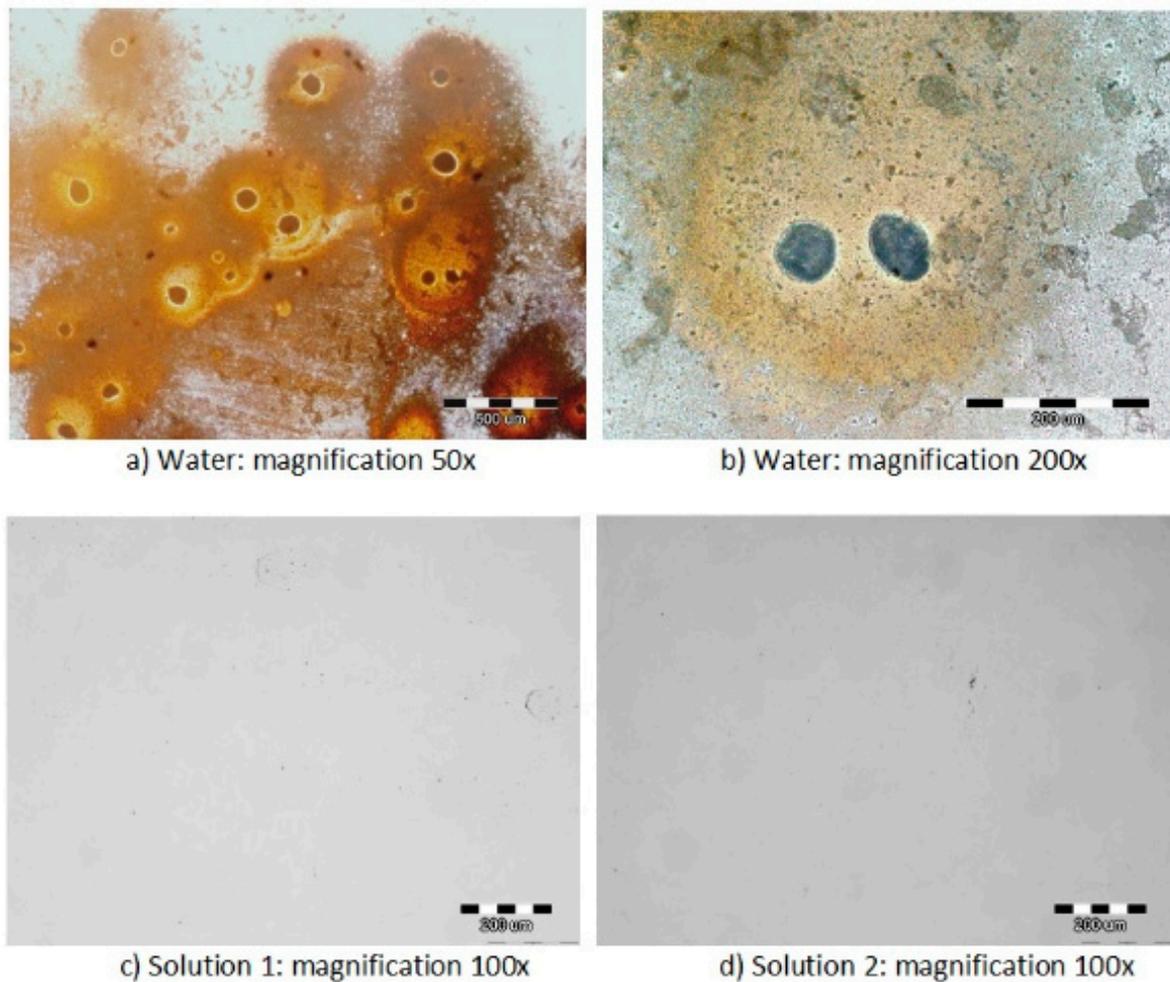

Figure 9. Microstructure of HTCS-130 hot work tool steel in: (**a**) water (magnification 50×, (**b**) water (magnification 200×), (**c**) solution 1 (magnification 100×), and (**d**) solution 2 (magnification 100×).

4. Conclusions

- According to the thermodynamic calculations, the segregation of individual phases at certain temperatures was found. From the obtained data, the segregation of carbides of type M_6C, MC, M_2C, and $M_{23}C_6$ was visible.
- By measuring the potential of the open circuit, negative values of the open circuit potential for the sample were obtained after testing in water. Better values were recorded for the sample tested in distilled water solution with the addition of inhibitor.
- The formation of a thicker protective layer on the surface of the sample after testing in solution 1 was established using the method of electrochemical impedance spectroscopy. This was evidenced by the higher amounts of oxide resistance R_{ox} oxide and charge transfer resistance R_{ct} of the sample exposed in solution 1.
- The potentiodynamic polarisation method showed a lower corrosion rate of the sample after testing in solution 1. The results obtained using the Tafel extrapolation method confirmed the better resistance of the sample during contact with the inhibitor.

- The lowest amounts of R_{ox} and R_{ct} were recorded for the sample tested in water. As a result, surface damage in the form of pits occurred. The resulting damage is characteristic in the Fe area. Areas where carbide phases were present were less affected by corrosion. No changes were observed on the recorded microstructures of the sample after testing in solution 1 and solution 2.
- SEM and EDS analysis confirmed the presence of tungsten and molybdenum elements. Tungsten and molybdenum form carbides of the Mo_6C and W_6C type. The obtained element analyses coincide with the obtained printout of the carbide segregation using the Thermo-Calc method.
- The tested steel can be classified into a very-high-quality group of tool steels for hot work. Based on the studies performed, however, the results suggest that the sample showed much better stability in solutions 1 and 2. The obtained result indicates that the commercial inhibitor VCI 379/611 has high efficiency, especially when it was tested on the sample in solution 1. Due to its effectiveness, it is considered a fully applicable agent for corrosion protection of tool steel HTCS-130 intended for hot work.

References

1. Krauss, G. *Steels: Processing, Structure, and Performance*; ASM International: Materials Park, OH, USA, 2015.
2. Bhadeshia, H.K.D.H.; Honeycombe, R.W.K. *Steels Microstructure and Properties*, 3rd ed.; Elsevier Ltd.: Amsterdam, The Netherlands, 2006.
3. Bhadeshia, H.K.D.H.; Honeycombe, R.W.K. *Steels Microstructure and Properties*, 4th ed.; Elsevier Ltd.: Amsterdam, The Netherlands, 2017.
4. Durand-Charre, M. *Microstructure of Steels and Cast Irons, Engineering Materials and Processes*; Springer: Berlin/Heidelberg, Germany, 2003.
5. Totten, G.E. *Steel Heat Treatment: Metallurgy and Technologies*; CRC Press: Boca Raton, FL, USA, 2006.
6. Mesquita, R.A.; Michael, K.; Schneider, R. *Tool Steels: Properties and Performance*; CRC Press: Boca Raton, FL, USA, 2017.
7. Sunulahpašić, R.; Oruč, M. *Tool Steels and Other Tool Materials (in Bosnian)*; University of Zenica Faculty of Metallurgy and Technology: Zenica, Bosnia and Herzegovina, 2019.
8. Bryson, W.E. *Heat Treatment, Selection and Application of Tool Steels*, 2nd ed.; Hanser Publications: Cincinnati, OH, USA, 2013.
9. Revie, R.W.; Uhlig, H.H. *Corrosion and Corrosion Control: An Introduction to Corrosion Science and Engineering*, 4th ed.; A John Wiley & Sons, INC., Publication: Hoboken, NJ, USA, 2008.
10. Bahadori, A. *Corrosion and Materials Selection*; John Wiley & Sons, Ltd: Chichester, UK, 2014.
11. During, E.D.D. *Corrosion Atlas, A Collection of Illustrated Case Histories*, 3rd ed.; Elsevier Ltd.: Amsterdam, The Netherlands, 2018.

12. Popov, N.B. *Corrosion Engineering Principles and Solved Problems*; Elsevier Ltd.: Amsterdam, The Netherlands, 2015.

13. Pedeferri, P. *Corrosion Science and Engineering*; Springer: Cham, Switzerland, 2018.

14. May, M. Corrosion behavior of mild steel immersed in different concentrations of NaCl solutions. *J. Sebpa Univ. (Pure Appl. Sci.)* **2016**, *15*, 1–12.

15. Fekry, A.M.; Ameer, M.A. Electrochemical investigation of corrosion and hydrogen evolution rate of mild steel in sulphuric acid solution. *Int. J. Hydrogen Energ.* **2011**, *36*, 11207–11215. [CrossRef]

16. Chen, R.Y.; Yuen, W.Y.D. Review of the high-temperature oxidation of iron and carbon steels in air or oxygen. *Oxid. Met.* **2003**, *59*, 433–468. [CrossRef]

17. Saunders, S.R.J.; Monteiro, M.; Rizzo, F. The oxidation behaviour of metals and alloys at high temperatures in atmospheres containing water vapour: A review. *Prog. Mater. Sci.* **2008**, *53*, 775–837. [CrossRef]

18. Abdel-Gaber, A.M.; Abd-El-Nabey, B.A.; Sidahmed, I.M.; El-Zayady, A.M.; Saadawy, M. Inhibitive action of some plant extracts on the corrosion of steel in acidic media. *Corros. Sci.* **2006**, *48*, 2765–2779. [CrossRef]

19. Yaro, A.S.; Hameed, K.W.; Khadom, A.A. Study for prevention of steel corrosion by sacrificial anode cathodic protection. *Theor. Found. Chem. Eng.* **2013**, *47*, 266–273. [CrossRef]

20. Franceschi, M.; Pezzato, L.; Settimi, A.G.; Gennari, C.; Pigato, M.; Polyakova, M.; Konstantinov, D.; Brunelli, K.; Dabalá, M. Effect of different austempering heat treatments on corrosion properties of high-silicon steel. *Mater* **2021**, *14*, 288. [CrossRef] [PubMed]

21. Meng, Y.; Sugiyama, S.; Yanagimoto, J. Microstructural evolution during partial melting and semisolid forming behaviors of two hot-rolled Cr–V–Mo tool steels. *J. Mater. Process. Technol.* **2015**, *225*, 203–212. [CrossRef]

22. Kaschnitz, E.; Hofer, P.; Funk, W. Thermophysical properties of a hot-work tool-steel with high thermal conductivity. *Int. J. Thermophys.* **2013**, *34*, 843–850. [CrossRef]

23. Ko, D.C.; Kim, S.; Kim, G.; Kim, B.; Kim, M. Influence of microstructure on galling resistance of cold-work tool steels with different chemical compositions when sliding against ultra-high-strength steel sheets under dry condition. *Wear* **2015**, *338*, 362–371. [CrossRef]

24. Sohar, C.R. *Lifetime Controlling Defects in Tool Steels*; Springer: Berlin, Germany, 2011.

25. Martin, J.W. *Concise Encyclopedia of the Structure of Materials*; Elsevier Ltd.: Amsterdam, The Netherlands, 2007; pp. 442–447.

26. Banerjee, M.K. Physical metallurgy of tool steels. In *Reference Module in Materials Science and Materials Engineering*; Elsevier Ltd.: Amsterdam, The Netherlands, 2018.

27. Roberts, G.; Krauss, G.; Kennedy, R. *Tool Steels*, 5th ed.; ASM International: Materials Park, OH, YSA, 1998.

28. Corrêa, J.G.; Schroeter, R.B.; Machado, Á.R. Tool life and wear mechanism analysis of carbide tools used in the machining of martensitic and supermartensitic stainless steels. *Tribol. Int.* **2017**, *105*, 102–117. [CrossRef]

29. Kim, H.; Kang, J.; Son, D.; Lee, T.; Cho, K. Evolution of carbides in cold-work tool steels. *Mater. Charact.* **2015**, *107*, 376–385. [CrossRef]

30. Yilbas, B.S.; Toor, I.; Malik, J.; Patel, F. Laser gas assisted treatment of AISI H12 tool steel and corrosion properties. *Opt. Lasers. Eng.* **2014**, *54*, 8–13. [CrossRef]

31. Szumera, J. *The Tool Steel Guide*; Industrial Press Inc.: New York, NY, USA, 2003.

32. Saunders, N.; Miodownik, A.P. *CALPHAD (Calculation of Phase Diagrams): A Comprehensive Guide*; Pergamon: Oxford, NY, USA, 1998; Volume 1.

33. Lukas, H.; Fries, S.G.; Sundman, B. *Computational Thermodynamics the Calphad Method*; Cambridge University Press: Cambridge, UK, 2007.

34. Brajčinović, S.; Begić Hadžipašić, A.; Slokar Benić, L.J. Influence of medium on corrosion and microstructural properties of K110 tool steel for cold work. In Proceedings of the Metal 2020: 29th International Conference on Metallurgy and Materials, Brno, Češka, 20–22 May 2020; pp. 816–821. [CrossRef]

35. Brajčinović, S.; Begić Hadžipašić, A.; Medved, J.; Kožuh, S. Influence of medium on corrosion and microstructural properties of HTCS-130 tool steel for hot work. In Proceedings of the 18th International Foundrymen Conference Coexistence of material science and sustainable technology in economic growth, Sisak, Croatia, 15–17 May 2019; Dolić, N., Zovko Brodarac, Z., Begić Hadžipašić, A., Eds.; University of Zagreb Faculty of Metallurgy: Sisak, Croatia; pp. 188–205.

36. Perez, N. *Electrochemistry and Corrosion Science*; Kluwer Academic Publishers: Boston, MA, USA, 2004.

37. Schütze, M.; Roche, M.; Bender, R. *Corrosion Resistance of Steels, Nickel Alloys and Zinc in Aqueous Media*; Dechema: Frankfurt, Germany, 2016.

38. Gassama, D.; Aziz Diagne, A.; Yade, I.; Fall, M.; Faty, S. Investigations on the corrosion of constructional steels in different aqueous and simulated atmospheric environments. *Bull. Chem. Soc. Ethiop.* **2015**, *29*, 299–310. [CrossRef]

39. Vander Voort, G.F. Metallographic Techniques for Tool Steels. In *ASM Handbook: Metallography and Microstructures*; ASM International: Materials Park, OH, USA, 2004; Volume 9.

40. Balaško, T.; Burja, J.; Medved, J. High-temperature oxidation of four hot-work tool steels. *Mater. Tehnol.* **2018**, *52*, 775–780. [CrossRef]